Journal of Sound and Vibration 329 (2010) 1523–1535

Contents lists available at ScienceDirect

Journal of Sound and Vibration

journal homepage: www.elsevier.com/locate/jsvi

3-D vibration analysis of circular rings with sectorial cross-sections

D. Zhou [a,*], Y.K. Cheung [b], S.H. Lo [b]

[a] College of Civil Engineering, Nanjing University of Technology, Xinmofan Road, Nanjing 210009, People's Republic of China
[b] Department of Civil Engineering, The University of Hong Kong, Porkfulam Road, Hong Kong, People's Republic of China

ARTICLE INFO

Article history:
Received 31 March 2009
Received in revised form
19 October 2009
Accepted 1 November 2009
Handling Editor: L.G. Tham

ABSTRACT

The free vibration characteristics of circular rings with sectorial cross-section are studied based on the three-dimensional (3-D), small strain, linear elasticity theory. The complete vibration spectrum has been obtained by using the Ritz method. A set of three-dimensional orthogonal coordinates composing of the polar coordinates (r,θ) at the origin of the sectorial cross-section and circumferential coordinate φ around the ring is developed to describe the variables in the analysis. Each of the displacement components is taken as a triplicate series: two Chebyshev polynomial series, respectively, about the r and θ coordinates, and a trigonometric series about the φ coordinate. Frequency parameters and vibration mode shapes are computed by means of the displacement-based extremum energy principle. Upper bound convergence of the first eight frequency parameters accurate to at least five significant figures is presented. The effect of radius ratio, subtended angle, and initial slope angle on frequency parameters is investigated in detail. All major modes such as flexural modes, thickness-shear modes, stretching modes, and torsional modes, etc. are presented in the paper. The present results may serve as a benchmark reference to validate the accuracy of various approximate theories and other computational techniques for the vibration of circular rings.

1. Introduction

Rings as basic structural elements can find their applications in civil, mechanical, aircraft, and marine engineering such as gyroscopes, springs, stiffness and tires, etc. The study on vibration characteristics of rings is very important because they commonly have to bear various dynamic loads.

Reviewing published literatures, one can find that most studies on ring vibrations are based on the one-dimensional beam theories [1–3]. Comparing to the straight beams, the governing equations of rings are more complicated and to obtain their solutions is more difficult because of the initial curvature of rings. For rings with symmetric cross-sections and material symmetry about its centreline plane, the vibrations can be divided into in-plane and out-of-plane ones, which could be separately solved [4–9]. For rings with asymmetric cross-section, the in-plane and out-of-plane vibrations are coupled [10,11].

It is well known that the exact elasticity theory does not rely on any hypotheses involving the kinematics of deformation. Using the three-dimensional (3-D) elasticity theory, a complete vibration spectrum of structures can be provided, which cannot otherwise be predicted by the approximate theories. Such an analysis not only provides realistic results but also allows overall physical insights. Although the 3-D vibrations of circular rings with circular and rectangular

* Corresponding author.
E-mail address: dingzhou57@yahoo.com (D. Zhou).

0022-460X/$ - see front matter © 2009 Elsevier Ltd. All rights reserved.
doi:10.1016/j.jsv.2009.11.004

cross-sections have been studied [12–16], few researchers studied the 3-D vibrations of circular rings with asymmetric cross-sections. Using simple geometric polynomials as the admissible functions of every displacement components, So and Leissa [17] analyzed 3-D vibrations of thick circular rings with square cross-sections rotated 45° from the revolution axis using the Ritz method. Kang and Leissa [18] presented a 3-D vibration analysis for thick, circular rings with an isosceles trapezoidal or triangular cross-section by the Ritz method. Moreover, Kang and Leissa [19] studied the 3-D vibration of rings with an elliptical cross-section using the Ritz method.

In this paper, the Ritz method is used to study the three-dimensional free vibration of circular rings with sectorial cross-sections. A set of orthogonal coordinates, a combination of the polar coordinate (r,θ) on the origin of each sectorial cross-section and the circumferential coordinate φ around the ring are developed to describe the displacements, strains and stresses. The displacement components are taken to be u, v and w in r, θ and φ coordinates. The corresponding stress and strain components are ε_r, ε_θ, ε_φ and $\gamma_{r\theta}$, $\gamma_{r\varphi}$, $\gamma_{\theta\varphi}$. Each of displacement components is expressed as a product of three separable series: the duplicate sets of Chebyshev polynomial series, respectively, about the r and θ coordinates and a set of trigonometric series about the φ coordinate. The eigenfrequencies and mode shapes are numerically calculated through the energy optimization process.

2. Basic formulations

Consider a ring with the sectorial cross-section, as shown in Fig. 1. The origin of the sectorial cross-section forms a circle (the dash line in the figure) whose radius is R. The initial slope angle (the angle between the coordinates x_φ and x_θ) and the subtended angle (the sector angle) of the cross-section are θ_0 and θ_1, respectively. A combination of the polar coordinates (r,θ) at the origin of each sectorial cross-section and the circumferential coordinate φ around the ring is developed to describe displacements, strains and stresses. The polar coordinates describe the variations within the cross-section and the circumferential coordinate describes those quantities along the direction normal to the cross-section. It is obvious that the three-dimensional coordinates (r,θ,φ) form an orthogonal set. The transformation relations between the Cartesian coordinates (x,y) and the present curved orthogonal coordinates (r,θ,φ) are given as follows:

$$x=[R+r\cos(\theta+\theta_0)]\cos\varphi;\quad y=[R+r\cos(\theta+\theta_0)]\sin\varphi;\quad z=r\sin(\theta+\theta_0) \tag{1}$$

where the coordinate θ begins from the axis x_θ.

Let u, v and w be respectively the displacement component in the r, θ and φ direction. The corresponding stress and strain components are respectively ε_r, ε_θ, ε_φ and $\gamma_{r\theta}$, $\gamma_{r\varphi}$, $\gamma_{\theta\varphi}$. The relations between the three-dimensional tensorial strains and displacement components in the curved orthogonal coordinate set are given by

$$\varepsilon_r=\frac{\partial u}{\partial r},\quad \varepsilon_\theta=\frac{1}{r}\frac{\partial v}{\partial\theta}+\frac{u}{r},$$

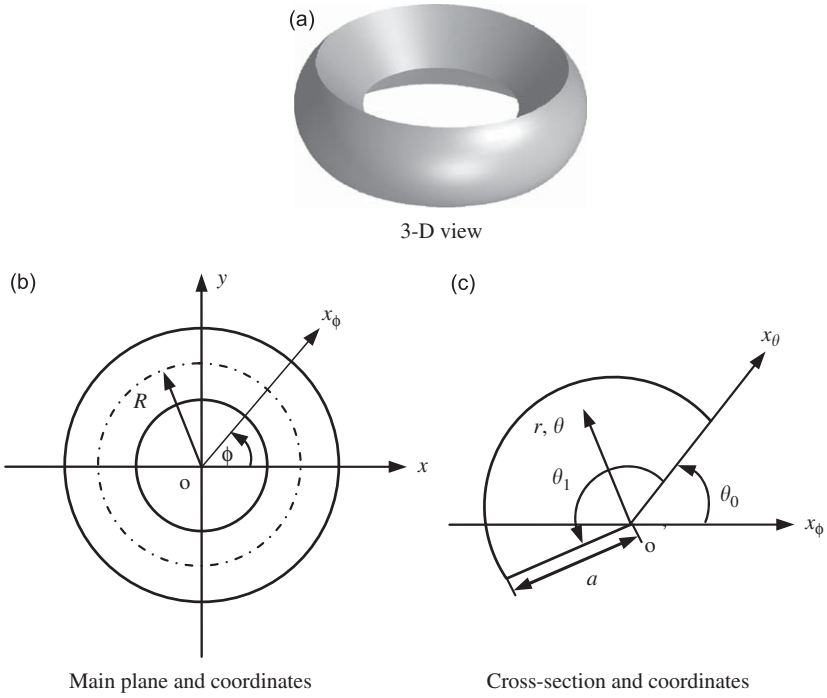

Fig. 1. A circular ring with sectorial cross-section: (a) 3-D view; (b) main plane and coordinates; (c) cross-section and coordinates.

$$\varepsilon_\varphi = \frac{1}{R+r\cos\theta}\frac{\partial w}{\partial \varphi} + \frac{\cos\theta}{R+r\cos\theta}u - \frac{\sin\theta}{R+r\cos\theta}v,$$

$$\gamma_{r\theta} = \frac{\partial v}{\partial r} - \frac{v}{r} + \frac{1}{r}\frac{\partial u}{\partial \theta}, \quad \gamma_{\theta\varphi} = \frac{1}{r}\frac{\partial w}{\partial \theta} + \frac{\sin\theta}{R+r\cos\theta}w + \frac{1}{R+r\cos\theta}\frac{\partial v}{\partial \varphi},$$

$$\gamma_{\varphi r} = \frac{1}{R+r\cos\theta}\frac{\partial u}{\partial \varphi} + \frac{\partial w}{\partial r} - \frac{\cos\theta}{R+r\cos\theta}w \tag{2}$$

From Eq. (1), the determinant of the Jacobian matrix of the coordinate system is given by

$$|J| = r[R+r\cos(\theta+\theta_0)] \tag{3}$$

Therefore, the strain energy V and the kinetic energy T of the ring undergoing free vibration are

$$V = (1/2)\int_0^{2\pi}\int_0^{\theta_1}\int_0^{a}[(\lambda+2G)\varepsilon_r^2 + 2\lambda\varepsilon_r\varepsilon_\theta + 2\lambda\varepsilon_r\varepsilon_\varphi + (\lambda+2G)\varepsilon_\theta^2 + 2\lambda\varepsilon_\theta\varepsilon_\varphi + (\lambda+2G)\varepsilon_\varphi^2 + G(\gamma_{r\theta}^2+\gamma_{\theta\varphi}^2+\gamma_{\varphi r}^2)]|J|\,\mathrm{d}r\,\mathrm{d}\theta\,\mathrm{d}\varphi,$$

$$T = (\rho/2)\int_0^{2\pi}\int_0^{\theta_1}\int_0^{a}(\dot{u}+\dot{v}+\dot{w})|J|\,\mathrm{d}r\,\mathrm{d}\theta\,\mathrm{d}\varphi \tag{4}$$

where ρ is the mass per unit volume, $\dot{u}$, $\dot{v}$ and $\dot{w}$ are the three-dimensional velocity components. Parameters λ and G are the Lamé constants for a homogeneous and isotropic material, which can be expressed in terms of the Young's modulus E and Poisson's ratio v by

$$\lambda = vE/[(1+v)(1-2v)], \quad G = E/[2(1+v)] \tag{5}$$

In free vibrations, the displacement components are expressed as

$$u = U(r,\theta,\varphi)\mathrm{e}^{\mathrm{i}\omega t}, \quad v = V(r,\theta,\varphi)\mathrm{e}^{\mathrm{i}\omega t}, \quad w = W(r,\theta,\varphi)\mathrm{e}^{\mathrm{i}\omega t} \tag{6}$$

where ω is the natural frequency of the ring and $\mathrm{i} = \sqrt{-1}$.

Considering the circumferential symmetry of the ring about the coordinate φ, the displacement functions are given by

$$U(r,\theta,\varphi) = \overline{U}(r,\theta)\cos(n\varphi), \quad V(r,\theta,\varphi) = \overline{V}(r,\theta)\cos(n\varphi),$$

$$W(r,\theta,\varphi) = \overline{W}(r,\theta)\sin(n\varphi) \tag{7}$$

where integer n is the circumferential wave number, i.e. $n = 0, 1, 2, 3, \ldots, \infty$ to ensure periodicity. It is obvious that n=0 denotes the axisymmetric vibration. In such a case, one has

$$U(r,\theta,\varphi) = \overline{U}(r,\theta), \quad V(r,\theta,\varphi) = \overline{V}(r,\theta), \quad W(r,\theta,\varphi) = 0 \tag{8}$$

Rotating the axes of symmetry, another set of displacement functions can be obtained, which corresponds to an interchange of $\cos(n\varphi)$ and $\sin(n\varphi)$ in Eq. (7). However, in such a case, n=0 corresponds to the torsional vibration, i.e.

$$U(r,\theta,\varphi) = 0, V(r,\theta,\varphi) = 0, W(r,\theta,\varphi) = \overline{W}(r,\theta) \tag{9}$$

Define the following dimensionless parameter and coordinates

$$\overline{R} = R/a, \quad \overline{r} = r/a, \quad \overline{\theta} = \theta/\theta_1 \tag{10}$$

Substituting Eqs. (6) and (7) into Eq. (4) gives

$$\begin{aligned} V_{\max} = {} & (G\theta_1 a/2)\int_0^1\int_0^1[(\overline{\lambda}+2)\overline{\varepsilon}_r^2 + 2\overline{\lambda}\overline{\varepsilon}_r\overline{\varepsilon}_\theta + 2\overline{\lambda}\overline{\varepsilon}_r\overline{\varepsilon}_\varphi + (\overline{\lambda}+2)\overline{\varepsilon}_\theta^2 + 2\overline{\lambda}\overline{\varepsilon}_\theta\overline{\varepsilon}_\varphi + (\overline{\lambda}+2)\overline{\varepsilon}_\varphi^2 + \overline{\gamma}_{r\theta}^2 + \overline{\gamma}_{\theta\varphi}^2 + \overline{\gamma}_{\varphi r}^2] \\ & \times[\overline{R}+\overline{r}\cos(\theta_1\overline{\theta}+\theta_0)]\overline{r}\,\mathrm{d}\overline{r}\,\mathrm{d}\overline{\theta}, \end{aligned}$$

$$T_{\max} = (\rho\theta_1 a^3\omega^2/2)\int_0^1\int_0^1(\Gamma_1\overline{U}^2 + \Gamma_1\overline{V}^2 + \Gamma_2\overline{W}^2)[\overline{R}+\overline{r}\cos(\theta_1\overline{\theta}+\theta_0)]\overline{r}\,\mathrm{d}\overline{r}\,\mathrm{d}\overline{\theta} \tag{11}$$

where

$$\overline{\lambda} = \frac{2v}{1-2v}, \quad \overline{\varepsilon}_r^2 = \Gamma_1\left(\frac{\partial\overline{U}}{\partial\overline{r}}\right)^2, \quad \overline{\varepsilon}_\theta^2 = \frac{\Gamma_1}{\overline{r}^2}\left[\frac{1}{\theta_1^2}\left(\frac{\partial\overline{V}}{\partial\overline{\theta}}\right)^2 + \frac{2}{\theta_1}\overline{U}\frac{\partial\overline{V}}{\partial\overline{\theta}} + \overline{U}^2\right],$$

$$\begin{aligned} \overline{\varepsilon}_\varphi^2 = {} & \frac{\Gamma_1}{[\overline{R}+\overline{r}\cos(\theta_1\overline{\theta}+\theta_0)]^2}[n^2\overline{W}^2 + 2n\cos(\theta_1\overline{\theta}+\theta_0)\overline{U}\overline{W} - 2n\sin(\theta_1\overline{\theta}+\theta_0)\overline{V}\overline{W} \\ & + \cos^2(\theta_1\overline{\theta}+\theta_0)\overline{U}^2 - \sin(2\theta_1\overline{\theta}+2\theta_0)\overline{U}\overline{V} + \sin^2(\theta_1\overline{\theta}+\theta_0)\overline{V}^2], \end{aligned}$$

$$\overline{\varepsilon}_r\overline{\varepsilon}_\theta = \frac{\Gamma_1}{\overline{r}}\left(\frac{1}{\theta_1}\frac{\partial\overline{U}}{\partial\overline{r}}\frac{\partial\overline{V}}{\partial\overline{\theta}} + \overline{U}\frac{\partial\overline{U}}{\partial\overline{r}}\right),$$

$$\overline{\varepsilon}_\theta\overline{\varepsilon}_\varphi = \frac{\Gamma_1}{\overline{r}[\overline{R}+\overline{r}\cos(\theta_1\overline{\theta}+\theta_0)]}\left[n\left(\frac{1}{\theta_1}\frac{\partial\overline{V}}{\partial\overline{\theta}}\overline{W}+\overline{U}\overline{W}\right)+\cos(\theta_1\overline{\theta}+\theta_0)\left(\frac{1}{\theta_1}\overline{U}\frac{\partial\overline{V}}{\partial\overline{\theta}}+\overline{U}^2\right)-\sin(\theta_1\overline{\theta}+\theta_0)\left(\frac{1}{\theta_1}\overline{V}\frac{\partial\overline{V}}{\partial\overline{\theta}}+\overline{U}\overline{V}\right)\right],$$

$$\overline{\varepsilon}_\varphi\overline{\varepsilon}_r = \frac{\Gamma_1}{\overline{R}+\overline{r}\cos(\theta_1\overline{\theta}+\theta_0)}\left[n\frac{\partial\overline{U}}{\partial\overline{r}}\overline{W}+\cos(\theta_1\overline{\theta}+\theta_0)\overline{U}\frac{\partial\overline{U}}{\partial\overline{r}}-\sin(\theta_1\overline{\theta}+\theta_0)\frac{\partial\overline{U}}{\partial\overline{r}}\overline{V}\right],$$

$$\gamma_{r\theta}^2 = \Gamma_1\left[\left(\frac{\partial\overline{V}}{\partial\overline{r}}\right)^2-\frac{2}{\overline{r}}\overline{V}\frac{\partial\overline{V}}{\partial\overline{r}}+\frac{2}{\theta_1\overline{r}}\frac{\partial\overline{U}}{\partial\overline{\theta}}\frac{\partial\overline{V}}{\partial\overline{r}}+\frac{1}{\overline{r}^2}\overline{V}^2-\frac{2}{\theta_1\overline{r}^2}\frac{\partial\overline{U}}{\partial\overline{\theta}}\overline{V}+\frac{1}{\theta_1^2\overline{r}^2}\left(\frac{\partial\overline{U}}{\partial\overline{\theta}}\right)^2\right],$$

$$\gamma_{\theta\varphi}^2 = \Gamma_2\left[\frac{1}{\theta_1^2\overline{r}^2}\left(\frac{\partial\overline{W}}{\partial\overline{\theta}}\right)^2+\frac{2(\sin(\theta_1\overline{\theta}+\theta_0)}{\theta_1\overline{r}[\overline{R}+\overline{r}\cos(\theta_1\overline{\theta}+\theta_0)]}\overline{W}\frac{\partial\overline{W}}{\partial\overline{\theta}}-\frac{n}{\theta_1}\overline{V}\frac{\partial\overline{W}}{\partial\overline{\theta}}+\frac{1}{[\overline{R}+\overline{r}\cos(\theta_1\overline{\theta}+\theta_0)]^2}(\sin^2\theta\overline{W}^2-2n\sin\theta\overline{V}\overline{W}+n^2\overline{V}^2)\right],$$

$$\gamma_{\varphi r}^2 = \Gamma_2\left[\left(\frac{\partial\overline{W}}{\partial\overline{r}}\right)^2-\frac{2}{\overline{R}+\overline{r}\cos(\theta_1\overline{\theta}+\theta_0)}\left(\cos(\theta_1\overline{\theta}+\theta_0)\overline{W}\frac{\partial\overline{W}}{\partial\overline{r}}+n\overline{U}\frac{\partial\overline{W}}{\partial\overline{r}}\right)+\frac{1}{[\overline{R}+\overline{r}\cos(\theta_1\overline{\theta}+\theta_0)]^2}(n^2\overline{U}^2+2n\cos(\theta_1\overline{\theta}+\theta_0)\overline{U}\overline{W}+\cos^2(\theta_1\overline{\theta}+\theta_0)\overline{W}^2)\right] \tag{12}$$

in which,

$$\Gamma_1 = \int_0^{2\pi}\cos^2 n\varphi\,\mathrm{d}\varphi = \begin{cases}2\pi & \text{if } n=0\\ \pi & \text{if } n\geq 1\end{cases},\quad \Gamma_2 = \int_0^{2\pi}\sin^2 n\varphi\,\mathrm{d}\varphi = \begin{cases}0 & \text{if } n=0\\ \pi & \text{if } n\geq 1\end{cases} \tag{13}$$

3. Ritz solution

According to Eq. (10), the Lagrangian energy functional Π is given by

$$\Pi = T_{\max} - V_{\max} \tag{14}$$

Assuming that the displacement functions $\overline{U}(\overline{r},\overline{\theta})$, $\overline{V}(\overline{r},\overline{\theta})$, and $\overline{W}(\overline{r},\overline{\theta})$ can be, respectively, expressed in terms of a finite series as

$$\overline{U}(\overline{r},\theta) = \sum_{i=1}^{I}\sum_{j=1}^{J}A_{ij}F_i(\overline{r})F_j(\overline{\theta}),\quad \overline{V}(\overline{r},\theta) = \sum_{l=1}^{L}\sum_{m=1}^{M}B_{lm}F_l(\overline{r})F_m(\overline{\theta}),$$

$$\overline{W}(\overline{r},\theta) = \sum_{p=1}^{P}\sum_{q=1}^{Q}C_{pq}F_p(\overline{r})F_q(\overline{\theta}) \tag{15}$$

where A_{ij}, B_{lm} and C_{pq} are the undetermined coefficients and I, J, L, M, P, and Q are the truncated orders of their corresponding series. It is well known that if $F_i(\overline{r})\,(i=1,2,3,\ldots,\infty)$ is a set of mathematically complete series, then the duplicate series in Eq. (15) is capable of accurately describing the three-dimensional displacement field of a ring. When sufficient terms are taken, the results could theoretically approach to the exact solutions as closely as desired.

In the present analysis, the admissible functions are taken to be the Chebyshev polynomials as follows [20]:

$$F_i(\overline{r}) = \cos[(i-1)\arccos(2\overline{r}-1)],\quad i=1,2,3,\ldots \tag{16}$$

For $F_j(\overline{\theta})\,(i=1,2,3,\ldots)$, one only needs to change the variable $\overline{r}$ in Eq. (16) into the variable $\overline{\theta}$. Due to the traction free surfaces for a closed ring, no displacement restraint should be considered when using the Ritz method to obtain solutions.

Minimizing functional (14) with respect to the coefficients of displacement functions, i.e.

$$\frac{\partial\Pi}{\partial A_{ij}} = 0,\quad \frac{\partial\Pi}{\partial B_{lm}} = 0,\quad \frac{\partial\Pi}{\partial C_{pq}} = 0 \tag{17}$$

leads to the following eigenfrequency equation:

$$\left[\begin{pmatrix}\mathbf{K}_{uu} & \mathbf{K}_{uv} & \mathbf{K}_{uw}\\ & \mathbf{K}_{vv} & \mathbf{K}_{vw}\\ Sym. & & \mathbf{K}_{ww}\end{pmatrix}-\Omega^2\begin{pmatrix}\mathbf{M}_{uu} & \mathbf{0} & \mathbf{0}\\ & \mathbf{M}_{vv} & \mathbf{0}\\ Sym. & & \mathbf{M}_{ww}\end{pmatrix}\right]\begin{Bmatrix}\mathbf{A}\\ \mathbf{B}\\ \mathbf{C}\end{Bmatrix} = \begin{Bmatrix}\mathbf{0}\\ \mathbf{0}\\ \mathbf{0}\end{Bmatrix},\quad \text{for } n\geq 1 \tag{18}$$

where $\Omega=\omega a\sqrt{\rho/G}$ and

$$\mathbf{A}=\begin{Bmatrix} A_{11}\\ A_{12}\\ \vdots\\ A_{1J}\\ A_{21}\\ \vdots\\ A_{2J}\\ \vdots\\ A_{I1}\\ \vdots\\ A_{IJ}\end{Bmatrix},\quad \mathbf{B}=\begin{Bmatrix} B_{11}\\ B_{12}\\ \vdots\\ B_{1L}\\ B_{21}\\ \vdots\\ B_{2L}\\ \vdots\\ B_{L1}\\ \vdots\\ B_{LM}\end{Bmatrix},\quad \mathbf{C}=\begin{Bmatrix} C_{11}\\ C_{12}\\ \vdots\\ C_{1Q}\\ C_{21}\\ \vdots\\ C_{2Q}\\ \vdots\\ C_{P1}\\ \vdots\\ C_{PQ}\end{Bmatrix} \tag{19}$$

$$\left[\begin{pmatrix}\mathbf{K}_{uu} & \mathbf{K}_{uw}\\ Sym. & \mathbf{K}_{ww}\end{pmatrix}-\Omega^2\begin{pmatrix}\mathbf{M}_{uu} & \mathbf{0}\\ Sym. & \mathbf{M}_{ww}\end{pmatrix}\right]\begin{Bmatrix}\mathbf{A}\\ \mathbf{C}\end{Bmatrix}=\begin{Bmatrix}\mathbf{0}\\ \mathbf{0}\end{Bmatrix},\quad n=0 \text{ for the axisymmetric vibration} \tag{20}$$

$$(\mathbf{K}_{vv}-\Omega^2\mathbf{M}_{vv})\mathbf{B}=\mathbf{0},\quad n=0 \text{ for the torsional vibration} \tag{21}$$

Elements in matrices K_{ij} and M_{ij} ($i,j=u,v,w$) are given in the Appendix.

4. Convergence and comparison of results

The eigenfrequencies provided by the Ritz method converge to the exact solutions in an upper bound manner. Theoretically, solution with any accuracy can be obtained by taking sufficient terms in Eq. (15). However, there is a limit to the number of terms actually used in the numerical computation. Therefore, it is important to understand the convergence rate and accuracy of the method. The convergence is presented for the first eight non-zero frequencies of a circular ring with sectorial cross-section when the radius ratio $\overline{R}=R/a=2.0$, the initial slope angle $\theta_0=-45^\circ$ and the subtended angle $\theta_1=270^\circ$. The frequency parameter $\Omega=\omega a\sqrt{\rho/G}$ for the axisymmetric and torsional vibrations with respect to different numbers of terms is given in Table 1. The frequency parameter Ω for the circumferential vibrations $n=1$ and $n=4$ with respect to the different numbers of terms is given in Fig. 2. For simplicity, equal numbers of terms of admissible functions are taken in displacement amplitude functions U, V and W although different numbers of terms among U, V and W might provide a more rapid convergence. All the numerical computations are performed in double precision and the piecewise Gaussian quadrature is used to obtain the matrices in Eq. (18). Six groups of terms from 10×10 to 20×20 with an increment 2 for each series are checked for convergence. It can be seen from Tables 1 and 2 that the first eight non-zero frequency parameters converge monotonically to five significant figures by using 18×18 terms for each vibration category. As the Chebyshev polynomial series used in the present analysis is a complete set, it can be concluded that these frequency parameters are "exact values" up to five digits. It is seen from Table 2 that the convergence rate is almost the same for $n=1$ and $n=4$, which means that the circumferential wave number n has no influence on the manner of convergence.

Table 1
The convergence of the first eight non-zero frequency parameters Ω_i ($i=1,2,\ldots,8$) of a circular ring with sectorial cross-section for axisymmetric and torsional vibrations for $\overline{R}=2.0$, $\theta_0=-45^\circ$ and $\theta_1=270^\circ$.

Terms	Ω_1	Ω_2	Ω_3	Ω_4	Ω_5	Ω_6	Ω_7	Ω_8
Axisymmetric vibration $n=0^a$								
10×10	0.48708	0.83858	1.4302	2.3203	2.8407	3.1691	3.4521	3.8413
12×12	0.48705	0.83853	1.4299	2.3199	2.8398	3.1688	3.4486	3.8165
14×14	0.48705	0.83852	1.4297	2.3199	2.8397	3.1688	3.4485	3.8153
16×16	0.48704	0.83851	1.4296	2.3199	2.8397	3.1688	3.4485	3.8153
18×18	0.48704	0.83850	1.4296	2.3198	2.8397	3.1688	3.4485	3.8153
20×20	0.48704	0.83850	1.4296	2.3198	2.8397	3.1688	3.4485	3.8153
Torsional vibration $n=0^t$								
10×10	1.6307	2.3181	3.1423	3.8736	3.9687	4.6881	4.9307	5.7907
12×12	1.6306	2.3180	3.1421	3.8719	3.9664	4.6718	4.9277	5.4537
14×14	1.6306	2.3180	3.1421	3.8719	3.9664	4.6706	4.9273	5.4182
16×16	1.6305	2.3180	3.1421	3.8719	3.9664	4.6706	4.9272	5.4164
18×18	1.6305	2.3180	3.1421	3.8719	3.9664	4.6706	4.9271	5.4163
20×20	1.6305	2.3180	3.1421	3.8719	3.9664	4.6706	4.9271	5.4163

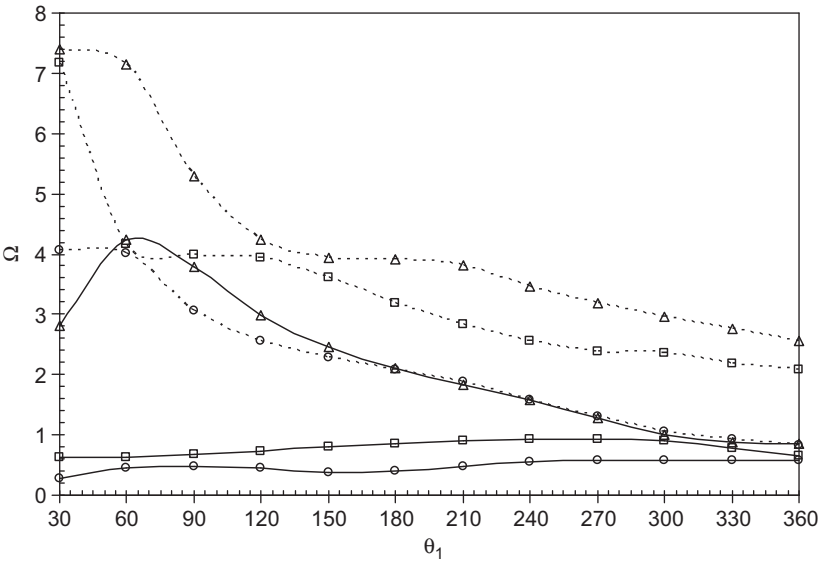

Fig. 2. The first three non-zero frequency parameters of axisymmetric and torsional vibrations for circular rings with initial slope angle θ_0=0° at radius ratio $\overline{R}=2.0$ against subtended angles varying from θ_1=30° to θ_1=360°, ○ the first frequency parameter; □ the second frequency parameter; △ the third frequency parameter, — axisymmetric vibration; ⋯ torsional vibration.

Table 2
The convergence of the first eight non-zero frequency parameters Ω_i (i=1,2,…,8) of a circular ring with sectorial cross-section for circumferential vibrations for $\overline{R}=2.0$, θ_0=−45° and θ_1=270°.

Terms	Ω_1	Ω_2	Ω_3	Ω_4	Ω_5	Ω_6	Ω_7	Ω_8
n=1								
10 × 10	0.69105	0.94855	1.3776	2.0644	2.2235	2.5557	2.8580	3.0670
12 × 12	0.69100	0.94855	1.3772	2.0643	2.2233	2.5557	2.8573	3.0669
14 × 14	0.69098	0.94854	1.3771	2.0642	2.2233	2.5556	2.8572	3.0669
16 × 16	0.69096	0.94854	1.3770	2.0642	2.2233	2.5556	2.8572	3.0669
18 × 18	0.69095	0.94854	1.3769	2.0642	2.2232	2.5556	2.8572	3.0669
20 × 20	0.69095	0.94854	1.3769	2.0642	2.2232	2.5556	2.8572	3.0669
n=4								
10 × 10	0.91113	1.3711	1.9222	2.3560	2.5569	2.7147	3.1930	3.3616
12 × 12	0.91105	1.3710	1.9220	2.3559	2.5566	2.7144	3.1920	3.3602
14 × 14	0.91102	1.3710	1.9219	2.3559	2.5566	2.7144	3.1919	3.3602
16 × 16	0.91101	1.3710	1.9219	2.3559	2.5565	2.7144	3.1919	3.3602
18 × 18	0.91100	1.3710	1.9219	2.3559	2.5565	2.7144	3.1919	3.3602
20 × 20	0.91100	1.3710	1.9219	2.3559	2.5565	2.7144	3.1919	3.3602

A comparison study of the present solutions with the finite element (FE) solutions is given in Table 3. The centerline radius of the ring is R=0.5 m and the cross-sectional radius of the ring is a=0.2 m. The material properties are $E=1.2\times10^{11}$ Pa (elasticity modulus), ρ=1850 kg/m^3 (density) and $\mu=0.3$ (Poisson's ratio). The subtended angle of the cross-section is fixed at θ_1=180°. Three different initial angles of the cross-section are considered respectively: θ_0=0°, −90°, 90°. The Solid95 element with 20 nodes in the commercial ANSYS program is used in the FE analysis. For θ_0=0°, 15 363 elements with 71 316 degrees of freedom are taken. For θ_0=−90°, 8783 elements with 43 035 degrees of freedom are taken and for θ_0=90°, 12 341 elements with 66 966 degrees of freedom are taken. In the present analysis, $I=J=12$ terms are taken. It can be seen from Table 3 that the present solutions are in good agreement with the FE solutions.

5. Numerical results

For thick circular rings, one-dimensional theories would bring considerable errors. In such a case, the three-dimensional elasticity analysis can provide more accurate results. Table 4 gives the first eight non-zero frequency parameters Ω_i (i=1,2,…,8) of five vibration categories ($n=0^a,0^t,1,2,3$) for thick rings with the sectorial cross-section, where the radius ratio $\overline{R}=R/a$ is equal to 2.0 and the subtended angle θ_1 of the cross-section is equal to 180°. Three different initial slope angles of the cross-section are considered: θ_0=−90°, 0°, 90°. Moreover, Table 5 gives the first eight non-zero frequency parameters Ω_i (i=1,2,…,8) of five vibration categories ($n=0^a,0^t,1,2,3$) for thick rings with the sectorial cross-section,

Table 3
The comparison of the present solutions with the finite element solutions for the first 10 natural frequencies ($f_i=\omega_i/2\pi$, i=1,2,…,10) for a ring with different initial angles.

Frequency sequence	θ_0=0°		θ_0=−90°		θ_0=90°	
	Present	FE	Present	FE	Present	FE
1	392.86 (2)	392.91	318.51 (2)	318.60	642.18 (2)	642.36
2	748.13 (2)	748.23	461.85 (2)	461.97	715.78 (2)	715.94
3	799.70 (0^a)	799.77	847.29 (3)	847.73	1611.9 (3)	1612.7
4	986.79 (3)	986.94	1205.0 (3)	1206.4	1699.6 (0^a)	1699.8
5	1239.1 (1)	1239.6	1288.3 (0^a)	1288.5	1700.2 (3)	1700.9
6	1675.6 (4)	1676.1	1388.4 (1)	1388.6	1944.5 (1)	1944.8
7	1716.7 (0^a)	1716.8	1417.0 (0^a)	1417.0	2014.6 (0^a)	2014.7
8	1755.1 (3)	1755.6	1508.9 (4)	1510.1	2704.7 (1)	2704.8
9	2091.5 (2)	2092.6	1790.4 (2)	1791.1	2711.1 (4)	2713.1
10	2137.0 (1)	2137.1	1953.6 (1)	1953.7	2744.2 (4)	2746.2

Note: The numbers within parentheses are the vibration categories of the ring.

Table 4
The first eight non-zero frequency parameters Ω_i (i=1,2,…,8) of five vibration categories for circular sectorial rings at three different slope angles with $\overline{R}=2.0$ and θ_1=180°.

n	Ω_1	Ω_2	Ω_3	Ω_4	Ω_5	Ω_6	Ω_7	Ω_8
θ_0=−90°								
0^a	0.61400	0.67142	2.0739	3.1499	3.1570	4.1086	4.3695	4.9648
0^t	1.9558	3.0660	3.9889	4.1813	5.2819	5.4860	6.3712	6.7979
1	0.65110	0.91466	2.0998	2.1124	3.0239	3.1742	3.2498	4.0035
2	0.17784	0.24870	0.84693	1.4077	2.1809	2.4761	2.9834	3.2258
3	0.46380	0.62469	1.1347	1.9345	2.3177	2.9147	3.0146	3.3123
θ_0=0°								
0^a	0.39972	0.85861	2.1035	3.1893	3.2458	4.1213	4.4435	4.9647
0^t	2.0874	3.1797	3.9202	4.3098	5.4056	5.4320	6.5057	6.7594
1	0.64494	0.99254	2.1283	2.3999	3.0130	3.2395	3.4662	3.9861
2	0.22150	0.43109	1.1034	1.4433	2.2817	2.9112	3.0138	3.2998
3	0.53090	0.96198	1.5923	1.9704	2.5342	3.0672	3.4114	3.5576
θ_0=90°								
0^a	0.87219	1.0511	2.1195	2.9836	3.2599	4.1159	4.4896	4.9606
0^t	1.7158	3.1933	3.8666	4.4176	5.2164	5.5437	6.6395	6.6636
1	0.98901	1.3550	2.0205	2.1218	2.8873	3.2595	3.5087	4.0511
2	0.41702	0.41853	1.4454	1.9806	2.1984	2.5997	2.9703	3.3054
3	0.94689	0.99057	2.0007	2.2038	2.8077	3.1853	3.2650	3.5057

where the radius ratio $\overline{R}=R/a$ is equal to 2.0 and the subtended angle θ_1 of the cross-section is equal to 90°. Five different initial slope angles of the cross-section are considered: θ_0=−45°, 0°, 90°, 135°, 225°. From Tables 4 and 5, one can see that for the same frequency order, the torsional vibration always gives the maximum frequency values while the circumferential vibration n=2 always gives the minimum frequency values. The effect of the initial slope angle on frequency parameters of circumferential vibrations is greatly larger than that on frequency parameters of torsional vibration. It can be seen that with the increase of frequency order, the effect of the initial slope angle θ_0 on frequency parameters decrease. However, this conclusion is not valid for the torsional vibration.

The effect of the subtended angle θ_1 on frequency parameter Ω is studied. The initial slope angle and the radius ratio of the rings are $\theta_0=0$ and $\overline{R}=2.0$, respectively. The first three non-zero frequency parameters for the axisymmetric and torsional vibrations and the first two non-zero frequency parameters for the circumferential vibrations n=1,2,3 are respectively given in Figs. 2 and 3. It is seen from Fig. 2 that the frequency parameters for the torsional vibration monotonically decrease with the increase of the subtended angle. When the subtended angle $\theta_1>150°$, the first frequency parameter for the torsional vibration approaches the third frequency parameter for the axisymmetric vibration. When the subtended angle θ_1=360°, the first two frequency parameters for the axisymmetric vibration are very close to each other. It can be seen from Fig. 3 that when the subtended angle θ_1=30°, the first frequency parameter for the circumferential vibration n=1 is very close to the second frequency parameter for the circumferential vibration n=3. When the subtended angle θ_1=360°, the first two frequency parameters for the circumferential vibration n=1 are very close to those of the circumferential vibration n=3. Within $180°\leq\theta_1\leq270°$ the second frequency parameters for the circumferential vibrations n=1 and n=3 are close to each other. Moreover, it is seen from Fig. 3 that the subtended angle corresponding to the maximum frequency parameter of each vibration categories are generally within $210°\leq\theta_1\leq270°$.

Table 5
The first eight non-zero frequency parameters Ω_i (i=1,2,…,8) of five vibration categories for circular sectorial rings at five different slope angles with $\overline{R}=2.0$ and θ_1=90°.

n	Ω_1	Ω_2	Ω_3	Ω_4	Ω_5	Ω_6	Ω_7	Ω_8
θ_0=−45°								
0^a	0.49146	0.62494	3.7832	4.4328	4.8921	5.0201	6.6086	6.6847
0^t	3.0086	4.0382	5.2323	6.8032	7.1590	7.4079	9.3245	9.5528
1	0.59383	0.86456	3.0823	3.7877	4.0859	4.4430	4.8823	5.0313
2	0.13941	0.15276	0.84508	1.3503	3.2847	3.8009	4.1857	4.5208
3	0.36957	0.40913	1.1539	1.8934	3.5761	3.8233	4.2610	4.7436
θ_0=0°								
0^a	0.48027	0.67476	3.7860	4.4553	4.8960	5.0177	6.6020	6.6828
0^t	3.0660	3.9889	5.2819	6.7879	7.1298	7.4517	7.3263	9.5921
1	0.60486	0.91835	3.1575	3.7929	4.0453	4.4577	4.8866	5.0307
2	0.15064	0.18905	0.89235	1.4223	3.4047	3.8135	4.1717	4.5134
3	0.39774	0.49286	1.2360	1.9849	3.7497	3.8520	4.2741	4.6914
θ_0=90°								
0^a	0.71818	1.0634	3.8134	4.5944	4.9067	4.9913	6.6143	6.6887
0^t	3.1933	3.8666	5.5437	6.6636	7.0300	7.7204	9.3147	9.8548
1	0.93613	1.3644	3.3944	3.8395	4.0566	4.5451	4.8737	5.0278
2	0.30872	0.42949	1.4345	2.0590	3.8141	3.9872	4.3844	4.5832
3	0.76713	1.0303	2.0164	2.8326	4.0986	4.3859	4.5129	4.6808
θ_0=135°								
0^a	0.96963	1.1772	3.8450	4.6234	4.8964	4.9760	6.6020	6.6948
0^t	3.2052	3.7674	5.5994	6.6440	6.9615	7.7916	9.3005	9.9010
1	1.1388	1.5359	3.4751	3.8145	4.0523	4.5452	4.8407	5.0201
2	0.42005	0.45000	1.6449	2.3066	3.9578	4.0969	4.4271	4.6199
3	1.0370	1.0748	2.2681	3.1282	4.1841	4.5312	4.6436	4.8592
θ_0=225°								
0^a	0.48276	0.82606	3.7914	4.5254	4.8982	5.0078	6.5951	6.6863
0^t	3.1796	3.8991	5.4148	6.7325	7.0778	7.5765	9.3260	9.7078
1	0.67385	1.0884	3.3247	3.8088	3.9873	4.5083	4.8801	5.0283
2	0.20264	0.29624	1.0736	1.6578	3.6836	3.8691	4.1931	4.5317
3	0.51983	0.73312	1.5277	2.2940	3.9295	4.1642	4.3703	4.6708

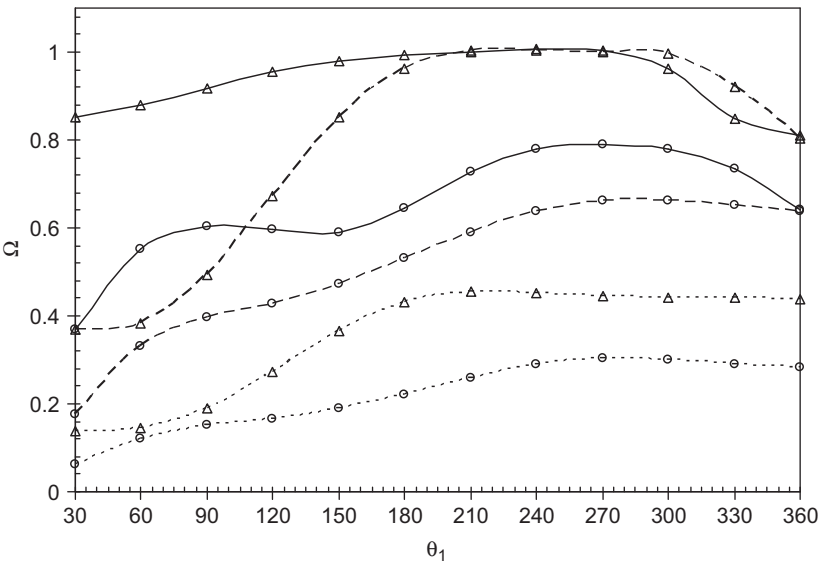

Fig. 3. The first two non-zero frequency parameters of circumferential vibrations for circular rings with the initial slope angle θ_0=0° at radius ratio $\overline{R}=2.0$ against subtended angles varying from θ_1=30° to θ_1=360°, ○ the first frequency parameter; △ the second frequency parameter, — n=1; ⋯ n=2; – – – n=3.

Numerical results show that there are three kinds of non-dimensional frequency parameters which converge to constant values with the increase of the radius ratio $\overline{R}$. Different vibration categories correspond to different non-dimensional frequency parameters which are, respectively, $\Omega=\omega a\sqrt{\rho/G}$, $\Gamma=\omega R\sqrt{\rho/G}$ and $\Lambda=\omega R\overline{R}\sqrt{\rho/G}$. Even for the

same vibration category, different orders can correspond to different frequency parameters. The relationships among the three kinds of frequency parameters are $\Gamma=\overline{R}\Omega$ and $\Lambda=\overline{R}\Gamma=\overline{R}^2\Omega$. The non-dimensional parameters corresponding to different vibration categories and frequency orders are given in Table 6, which are independent of the initial slope angle or the subtended angle of the cross-section.

The effect of radius ratio R/a on frequency parameters for five vibration categories n=0^a,0^t,1,2,3 are studied for a ring with the initial slope angle $\theta_0=-90^\circ$ and the subtended angle $\theta_1=180^\circ$. Three different frequency parameters Ω, Γ and Λ are used to describe the different vibration categories and different frequency orders, as given respectively in Figs. 4–6, where R/a is plotted along a logarithmic axis. It is seen from Figs. 4–6 that all the frequency parameters approach to constant values with the increase of the radius ratio R/a. The effect of the radius ratio R/a on frequency parameters is mainly limited to $0<R/a<10$. The smaller R/a, the larger is the effect of R/a on frequency parameters and the larger the circumferential number n, the larger is the effect of R/a on frequency parameters. It is seen from Fig. 4 that all frequency parameters monotonically decrease with the increase of the radius ratio R/a. The constant value of the first frequency parameter for the torsional vibration is the same as that of the third frequency parameter for the circumferential vibration n=1. The converged value of the third frequency parameter for the axisymmetric vibration is the same as that for the fourth frequency parameter for the circumferential vibration n=2. Moreover, the constant value of the second frequency parameter for the torsional vibration is the same as that of the fourth frequency parameter for the axisymmetric vibration. It is seen from Fig. 5 that the converged constant value of the first frequency parameter for the circumferential vibration n=1 is the same as that of the second frequency parameter for the axisymmetric vibration. Furthermore, it is seen from Figs. 5 and 6 that all the frequency parameters monotonically increase with the increase of the radius ratio R/a.

The first two mode shapes for the axisymmetric and torsional vibrations when R/a=0.2 are plotted in Fig. 7. It can be seen from Fig. 7 that the first axisymmetric mode clearly includes a rigid rotation of the cross-section whereas the second axisymmetric mode reflects the symmetric deformation of the cross-section in the θ direction. Moreover, the first torsional

Table 6
Converged values of frequency parameters with the increase of the radius ratio $\overline{R}$.

Vibration categories	Frequency orders	Convergent parameters
n=0^t	All	Ω
n=0^a	1, 2	Γ
	≥3	Ω
n=1	1, 2	Γ
	≥3	Ω
$n\geq 2$	1, 2	Λ
	3, 4	Γ
	≥5	Ω

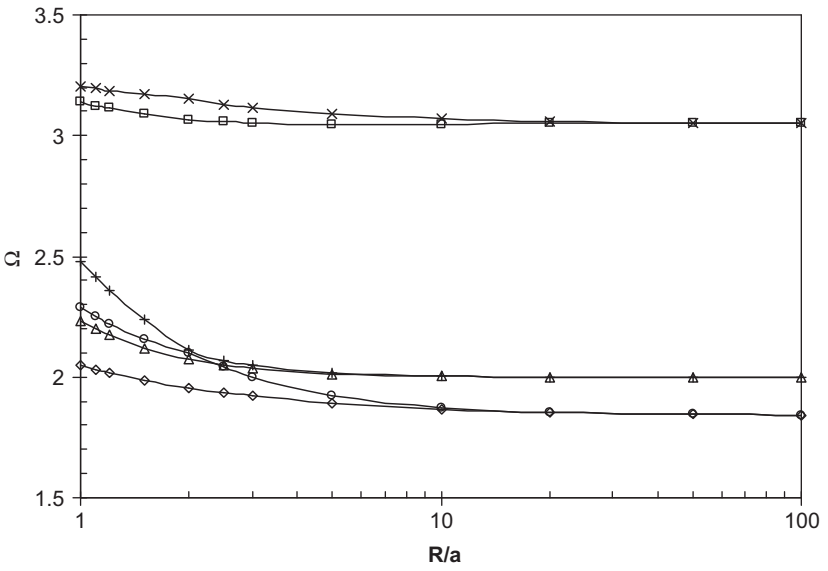

Fig. 4. Frequency parameter Ω of a circular ring with initial slope angle $\theta_0=-90^\circ$ and subtended angle $\theta_1=180^\circ$ against radius ratio R/a: ◇, first frequency of torsional vibration; □, second frequency of torsional vibration; △, third frequency of axisymmetric vibration; ×, fourth frequency of axisymmetric vibration; ○, third frequency of circumferential vibration n=1; +, fourth frequency of circumferential vibration n=1.

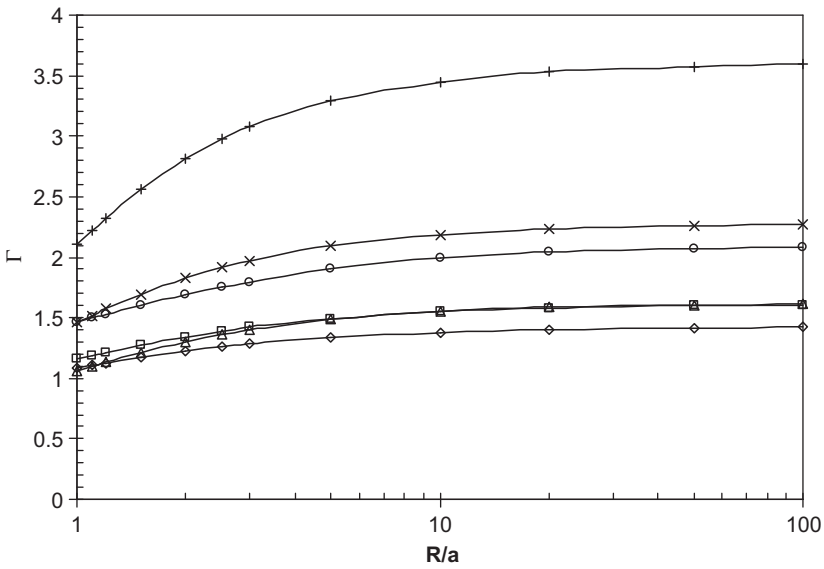

Fig. 5. Frequency parameter Γ of a circular ring with initial slope angle $\theta_0=-90^\circ$ and subtended angle $\theta_1=180^\circ$ against radius ratio R/a: ◇, first frequency of axisymmetric vibration; □, second frequency of axisymmetric vibration; △, first frequency of circumferential vibration $n=1$; ×, second frequency of circumferential vibration $n=1$; ○, third frequency of circumferential vibration $n=2$; +, fourth frequency of circumferential vibration $n=2$.

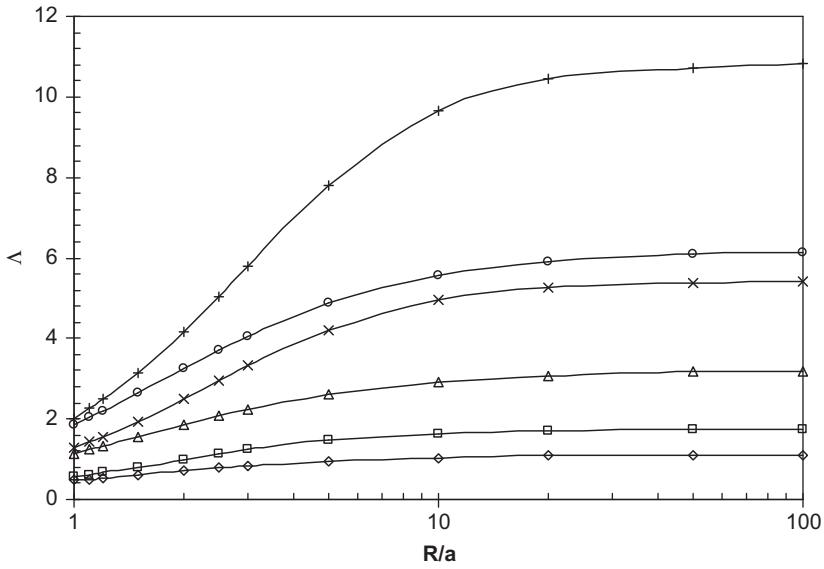

Fig. 6. Frequency parameter Λ of a circular ring with initial slope angle $\theta_0=-90^\circ$ and subtended angle $\theta_1=180^\circ$ against radius ratio R/a: ◇, first frequency of circumferential vibration $n=2$; □, second frequency of circumferential vibration $n=2$; △, first frequency of circumferential vibration $n=3$; ×, second frequency of circumferential vibration $n=3$; ○, first frequency of circumferential vibration $n=4$; +, second frequency of circumferential vibration $n=4$.

mode reflects the symmetric warping of the cross-section in the θ direction while second one reflects the antisymmetric warping. The first two mode shapes for the circumferential vibrations $n=1,2$ are plotted in Fig. 8. It is seen from Fig. 8 that the first mode for $n=1$ and the second mode for $n=2$ are antisymmetric about the coordinate θ whereas the second mode for $n=1$ and the first mode for $n=2$ are symmetric about the coordinate θ.

6. Conclusions

Based on the exact, small strain and linear elasticity theory, the three-dimensional vibration characteristics of closed rings with sectorial cross-section have been studied. The volume integrals for strain and kinetic energies have been formulated by developing a set of curved orthogonal coordinates. By means of the Ritz method, the governing eigenfrequency equations are derived through the minimization of the extremum of energy functional. The duplicate Chebyshev polynomial series are

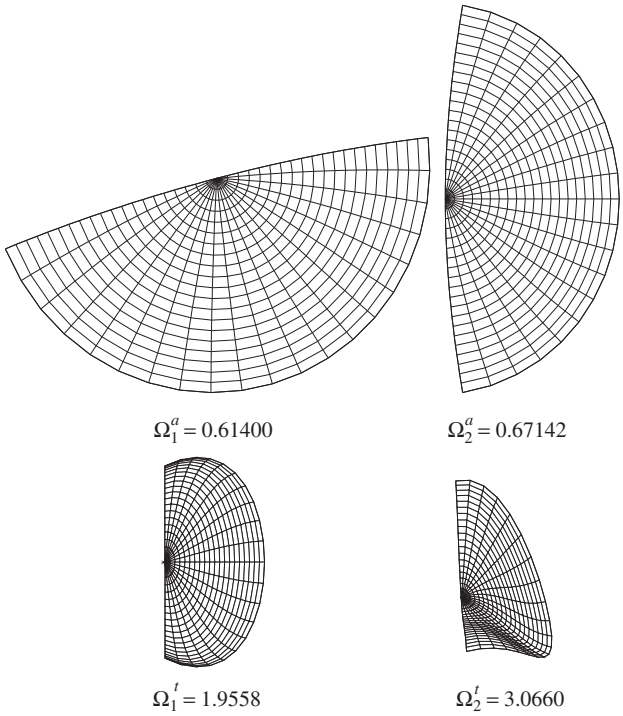

Fig. 7. The first two cross-sectional mode shapes of axisymmetric and torsional vibrations for a circular ring with radius ratio $\overline{R} = 2$, inertial slope angle $\theta_0 = -90^\circ$ and subtended angle $\theta_1 = 180^\circ$.

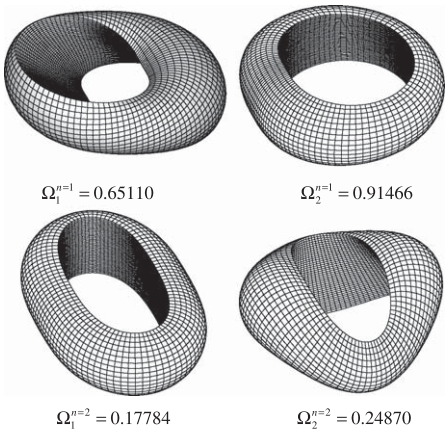

Fig. 8. The first two 3-D mode shapes of circumferential vibrations $n = 1$ and $n = 2$ for a circular ring with radius ratio $\overline{R} = 2$, inertial slope angle $\theta_0 = -90^\circ$ and subtended angle $\theta_1 = 180^\circ$.

taken as admissible functions for each displacement component. The convergence of the first eight frequency parameters has been examined, and accurate results to at least five significant figures have been obtained. The present analysis provides the complete vibration spectrum for the closed rings with sectorial cross-section. Through the parametric studies, the variations of frequency parameters versus the radius ratio, the initial slope angle and the subtended angle of cross-section are discussed. Accurate results for three-dimensional vibration analysis of thick rings with sectorial cross-section are presented for the first time, which could serve as valuable benchmark solutions for validating one-dimensional approximate theories and other less rigorous computational methods for the ring vibration problem.

Acknowledgment

The work described in this paper was supported by the CAS membership "Structural vibrations in three-dimensional solids" from The University of Hong Kong.

Appendix

The elements in K_{ij} and M_{ii} ($i,j=u,v,w$):

$$K_{uu}=\int_0^1\int_0^1\left\{\left[(\bar{\lambda}+2)\frac{\Gamma_1}{\bar{r}^2}+2\bar{\lambda}\frac{\Gamma_1\cos(\theta_1\bar{\theta}+\theta_0)}{\bar{r}[\bar{R}+\bar{r}\cos(\theta_1\bar{\theta}+\theta_0)]}+(\bar{\lambda}+2)\frac{\Gamma_1\cos^2(\theta_1\bar{\theta}+\theta_0)}{[\bar{R}+\bar{r}\cos(\theta_1\bar{\theta}+\theta_0)]^2}+\frac{\Gamma_2 n^2}{[\bar{R}+\bar{r}\cos(\theta_1\bar{\theta}+\theta_0)]^2}\right]\right.$$
$$\times F_i(\bar{r})F_{\bar{i}}(\bar{r})F_j(\bar{\theta})F_{\bar{j}}(\bar{\theta})+\bar{\lambda}\Gamma_1\left(\frac{1}{\bar{r}}+\frac{\cos(\theta_1\bar{\theta}+\theta_0)}{\bar{R}+\bar{r}\cos(\theta_1\bar{\theta}+\theta_0)}\right)[F_i(\bar{r})\dot{F}_{\bar{i}}(\bar{r})+\dot{F}_i(\bar{r})F_{\bar{i}}(\bar{r})]F_j(\bar{\theta})F_{\bar{j}}(\bar{\theta})$$
$$\left.+(\bar{\lambda}+2)\Gamma_1\dot{F}_i(\bar{r})\dot{F}_{\bar{i}}(\bar{r})F_j(\bar{\theta})F_{\bar{j}}(\bar{\theta})+\frac{\Gamma_1}{\theta_1^2\bar{r}^2}F_i(\bar{r})F_{\bar{i}}(\bar{r})\dot{F}_j(\bar{\theta})\dot{F}_{\bar{j}}(\bar{\theta})\right\}\bar{r}[\bar{R}+\bar{r}\cos(\theta_1\bar{\theta}+\theta_0)]\,\mathrm{d}\bar{r}\,\mathrm{d}\bar{\theta}$$

$$K_{vv}=\int_0^1\int_0^1\left\{\left[(\bar{\lambda}+2)\frac{\Gamma_1\sin^2(\theta_1\bar{\theta}+\theta_0)}{[\bar{R}+\bar{r}\cos(\theta_1\bar{\theta}+\theta_0)]^2}+\frac{\Gamma_1}{\bar{r}^2}+\frac{\Gamma_2 n^2}{[\bar{R}+\bar{r}\cos\cos(\theta_1\bar{\theta}+\theta_0)]^2}\right]\right.$$
$$\times F_l(\bar{r})F_{\bar{l}}(\bar{r})F_m(\bar{\theta})F_{\bar{m}}(\bar{\theta})-\bar{\lambda}\frac{\Gamma_1\sin(\theta_1\bar{\theta}+\theta_0)}{\theta_1\bar{r}[\bar{R}+\bar{r}\cos(\theta_1\bar{\theta}+\theta_0)]}F_l(\bar{r})F_{\bar{l}}(\bar{r})[F_m(\bar{\theta})\dot{F}_{\bar{m}}(\bar{\theta})+\dot{F}_m(\bar{\theta})F_{\bar{m}}(\bar{\theta})]$$
$$+(\bar{\lambda}+2)\frac{\Gamma_1}{\theta_1^2\bar{r}^2}F_l(\bar{r})F_{\bar{l}}(\bar{r})\dot{F}_m(\bar{\theta})\dot{F}_{\bar{m}}(\bar{\theta})+\Gamma_1\dot{F}_l(\bar{r})\dot{F}_{\bar{l}}(\bar{r})F_m(\bar{\theta})]F_{\bar{m}}(\bar{\theta})$$
$$\left.-\frac{\Gamma_1}{\bar{r}}[F_l(\bar{r})\dot{F}_{\bar{l}}(\bar{r})+\dot{F}_l(\bar{r})F_{\bar{l}}(\bar{r})]F_m(\bar{\theta})F_{\bar{m}}(\bar{\theta})\right\}\bar{r}[\bar{R}+\bar{r}\cos(\theta_1\bar{\theta}+\theta_0)]\,\mathrm{d}\bar{r}\,\mathrm{d}\bar{\theta},$$

$$K_{ww}=\int_0^1\int_0^1\left\{\frac{1}{[\bar{R}+\bar{r}\cos(\theta_1\bar{\theta}+\theta_0)]^2}[(\bar{\lambda}+2)\Gamma_1 n^2+\Gamma_2]F_p(\bar{r})F_{\bar{p}}(\bar{r})F_q(\bar{\theta})F_{\bar{q}}(\bar{\theta})+\frac{\Gamma_1}{\theta_1^2\bar{r}^2}F_p(\bar{r})F_{\bar{p}}(\bar{r})\dot{F}_q(\bar{\theta})\dot{F}_{\bar{q}}(\bar{\theta})\right.$$
$$+\frac{\Gamma_2\sin(\theta_1\bar{\theta}+\theta_0)}{\theta_1\bar{r}[\bar{R}+\bar{r}\cos(\theta_1\bar{\theta}+\theta_0)]}F_p(\bar{r})F_{\bar{p}}(\bar{r})[F_q(\theta)\dot{F}_{\bar{q}}(\theta)+\dot{F}_q(\theta)F_{\bar{q}}(\theta)]+\Gamma_2\dot{F}_p(\bar{r})\dot{F}_{\bar{p}}(\bar{r})F_q(\theta)F_{\bar{q}}(\theta)$$
$$\left.-\frac{\Gamma_2\cos(\theta_1\bar{\theta}+\theta_0)}{\bar{R}+\bar{r}\cos(\theta_1\bar{\theta}+\theta_0)}[F_p(\bar{r})\dot{F}_{\bar{p}}(\bar{r})+\dot{F}_p(\bar{r})F_{\bar{p}}(\bar{r})]F_q(\bar{\theta})F_{\bar{q}}(\bar{\theta})\right\}\bar{r}[\bar{R}+\bar{r}\cos(\theta_1\bar{\theta}+\theta_0)]\,\mathrm{d}\bar{r}\,\mathrm{d}\bar{\theta},$$

$$K_{uv}=\int_0^1\int_0^1\left\{\bar{\lambda}\frac{\Gamma_1}{\bar{r}}\dot{F}_i(\bar{r})F_l(\bar{r})F_j(\bar{\theta})F_m(\bar{\theta})-\bar{\lambda}\frac{\Gamma_1\sin(\theta_1\bar{\theta}+\theta_0)}{\bar{R}+\bar{r}\cos(\theta_1\bar{\theta}+\theta_0)}\dot{F}_i(\bar{r})F_l(\bar{r})F_j(\bar{\theta})F_m(\bar{\theta})\right.$$
$$+\left[(\bar{\lambda}+2)\frac{\Gamma_1}{\bar{r}^2}+\bar{\lambda}\frac{\Gamma_1\cos(\theta_1\bar{\theta}+\theta_0)}{\bar{r}[\bar{R}+\bar{r}\cos(\theta_1\bar{\theta}+\theta_0)]}\right]F_i(\bar{r})F_l(\bar{r})F_j(\bar{\theta})F_m(\bar{\theta})$$
$$-\left[\bar{\lambda}\frac{\Gamma_1\sin(\theta_1\bar{\theta}+\theta_0)}{\bar{r}[\bar{R}+\bar{r}\cos(\theta_1\bar{\theta}+\theta_0)]}+(\bar{\lambda}+2)\frac{\Gamma_1\sin[2(\theta_1\bar{\theta}+\theta_0)]}{2[\bar{R}+\bar{r}\cos(\theta_1\bar{\theta}+\theta_0)]^2}\right]F_i(\bar{r})F_l(\bar{r})F_j(\bar{\theta})F_m(\bar{\theta})$$
$$\left.+\frac{\Gamma_1}{\theta_1\bar{r}}F_i(\bar{r})\dot{F}_l(\bar{r})\dot{F}_j(\bar{\theta})F_m(\bar{\theta})-\frac{\Gamma_1}{\bar{r}^2}F_i(\bar{r})\dot{F}_j(\bar{r})F_l(\bar{\theta})F_m(\bar{\theta})\right\}\bar{r}[\bar{R}+\bar{r}\cos(\theta_1\bar{\theta}+\theta_0)]\,\mathrm{d}\bar{r}\,\mathrm{d}\bar{\theta},$$

$$K_{uw}=\int_0^1\int_0^1\left\{\bar{\lambda}\frac{\Gamma_1 n^2}{\bar{R}+\bar{r}\cos(\theta_1\bar{\theta}+\theta_0)}F_i(\bar{r})F_p(\bar{r})F_j(\bar{\theta})F_q(\bar{\theta})\right.$$
$$+\left[\bar{\lambda}\frac{\Gamma_1 n}{\bar{r}[\bar{R}+\bar{r}\cos(\theta_1\bar{\theta}+\theta_0)]}+[(\lambda+2)\Gamma_1+\Gamma_2]\frac{n\cos(\theta_1\bar{\theta}+\theta_0)}{\bar{R}+\bar{r}\cos(\theta_1\bar{\theta}+\theta_0)}\right]F_i(\bar{r})F_p(\bar{r})F_j(\bar{\theta})F_q(\bar{\theta})$$
$$\left.-\frac{n\Gamma_2}{\bar{R}+\bar{r}\cos(\theta_1\bar{\theta}+\theta_0)}F_i(\bar{r})\dot{F}_p(\bar{r})F_j(\bar{\theta})F_q(\bar{\theta})\right\}\bar{r}[\bar{R}+\bar{r}\cos(\theta_1\bar{\theta}+\theta_0)]\,\mathrm{d}\bar{r}\,\mathrm{d}\bar{\theta},$$

$$K_{vw}=\int_0^1\int_0^1\left\{\bar{\lambda}\frac{\Gamma_1 n}{\theta_1\bar{r}[\bar{R}+\bar{r}\cos(\theta_1\bar{\theta}+\theta_0)]}F_l(\bar{r})F_p(\bar{r})\dot{F}_m(\bar{\theta})F_q(\bar{\theta})-[(\bar{\lambda}+2)\Gamma_1+\Gamma_2]\right.$$
$$\times\frac{n\sin(\theta_1\bar{\theta}+\theta_0)}{\bar{R}+\bar{r}\cos(\theta_1\bar{\theta}+\theta_0)}F_l(\bar{r})F_p(\bar{r})F_m(\bar{\theta})F_q(\bar{\theta})-\frac{n\Gamma_2}{\theta_1\bar{r}[\bar{R}+\bar{r}\cos(\theta_1\bar{\theta}+\theta_0)]}$$
$$\left.\times F_l(\bar{r})F_p(\bar{r})F_m(\bar{\theta})\dot{F}_q(\bar{\theta})\right\}\bar{r}[\bar{R}+\bar{r}\cos(\theta_1\bar{\theta}+\theta_0)]\,\mathrm{d}\bar{r}\,\mathrm{d}\bar{\theta},$$

$$M_{uu}=\int_0^1\int_0^1\{F_i(\bar{r})F_{\bar{i}}(\bar{r})F_j(\bar{\theta})F_{\bar{j}}(\bar{\theta})\}\bar{r}[\bar{R}+\bar{r}\cos(\theta_1\bar{\theta}+\theta_0)]\,\mathrm{d}\bar{r}\,\mathrm{d}\bar{\theta},$$

$$M_{vv}=\int_0^1\int_0^1\{F_l(\bar{r})F_{\bar{l}}(\bar{r})F_m(\bar{\theta})F_{\bar{m}}(\bar{\theta})\}\bar{r}[\bar{R}+\bar{r}\cos(\theta_1\bar{\theta}+\theta_0)]\,\mathrm{d}\bar{r}\,\mathrm{d}\bar{\theta},$$

$$M_{ww} = \int_0^1 \int_0^1 \{F_p(\overline{r})F_{\overline{p}}(\overline{r})F_q(\overline{\theta})F_{\overline{q}}(\overline{\theta})\}\overline{r}[\overline{R}+\overline{r}\cos(\theta_1\overline{\theta}+\theta_0)]\,\mathrm{d}\overline{r}\,\mathrm{d}\overline{\theta},$$

$$i,\overline{i} = 1,2,3,\ldots,I, \quad j,\overline{j} = 1,2,3,\ldots,J, \quad l,\overline{l} = 1,2,3,\ldots,L,$$

$$m,\overline{m} = 1,2,3,\ldots,M, \quad p,\overline{p} = 1,2,3,\ldots,P, \quad q,\overline{q} = 1,2,3,\ldots,Q$$

References

[1] A.E.H. Love, On the vibrations of an elastic circular ring (Abstract), *Proceedings of the London Mathematical Society* 24 (1892–1893) 118–120.
[2] R. Hoppe, The bending vibration of a circular ring, *Crelle Journal of Mathematics* 73 (1871) 158–168.
[3] P. Chidamparan, A.W. Leissa, Vibrations of planar curved beams, rings and arches, *Applied Mechanics Reviews* 46 (1993) 467–483.
[4] S.S. Rao, V. Sundararajan, In-plane flexural vibrations of circular rings, *Journal of Applied Mechanics—ASME* 36 (1969) 620–625.
[5] L.L. Philipson, On the role of extension in the flexural vibration of ring, *Journal of Applied Mechanics—ASME* 23 (1956) 364–366.
[6] J. Kirkhope, Simple frequency expression of in-plane vibration of thick circular rings, *Journal of the Acoustical Society of America* 59 (1976) 86–89.
[7] J. Kirkhope, Out-plane vibration of thick circular ring, *Journal of Engineering Mechanics—ASCE* 102 (1976) 239–247.
[8] J.S. Bakshi, W.R. Callahan, Flexural vibrations of a circular ring when transverse shear and rotary inertia are considered, *Journal of the Acoustical Society of America* 40 (1966) 372–375.
[9] C.S. Tang, C.W. Bert, Out-of-plane vibrations of thick rings, *International Journal of Solids and Structures* 23 (1987) 175–185.
[10] M.Y. Kim, N.I. Kim, B.C. Min, Analytical and numerical study on spatial free vibration of non-symmetric thin-walled curved beams, *Journal of Sound and Vibration* 258 (2002) 595–618.
[11] N.I. Kim, M.Y. Kim, Spatial free vibration of shear deformable circular curved beams with non-symmetric thin-walled sections, *Journal of Sound and Vibration* 276 (2006) 245–271.
[12] O. Taniguchi, M. Endo, An approximate formula for the flexural vibration of a ring of rectangular cross section, *Bulletin of the JSME* 14 (1971) 348–354.
[13] M. Endo, Flexural vibrations of a ring with arbitrary cross-section, *Bulletin of JSME* 15 (1972) 446–544.
[14] R.K. Singal, K. Williams, A theoretical and experimental study of vibrations of thick circular cylindrical shells and rings, *Journal of Vibration, Acoustics and Stress Reliability Design* 110 (1988) 533–537.
[15] D. Zhou, Y.K. Cheung, S.H. Lo, F.T.K. Au, 3-D vibration analysis of solid and hollow circular cylinders via Chebyshev–Ritz method, *Computer Methods in Applied Mechanics and Engineering* 192 (2003) 1575–1589.
[16] D. Zhou, F.T.K. Au, S.H. Lo, Y.K. Cheung, Three-dimensional vibration analysis of a torus with circular cross-section, *Journal of the Acoustical Society of America* 112 (2002) 2831–2839.
[17] J. So, A.W. Leissa, Free vibrations of thick hollow circular cylinders from three-dimensional analysis, *Journal of Vibration and Acoustics* 119 (1997) 89–95.
[18] J.H. Kang, A.W. Leissa, Three-dimensional vibrations of thick, circular rings with isosceles trapezoidal and triangular cross-sections, *Journal of Vibration and Acoustics* 122 (2000) 132–139.
[19] J.H. Kang, A.W. Leissa, Natural frequencies of thick, complete, circular rings with an elliptical or circular cross-section from a three-dimensional theory, *Archive of Applied Mechanics* 75 (2006) 425–439.
[20] L. Fox, I.B. Parker, *Chebyshev Polynomials in Numerical Analysis*, Oxford University Press, London, 1968.